Biophysical Journal, Volume 99

Supporting Material

Scrutinizing Molecular Mechanics Force Fields on the Microsecond Timescale With NMR Data

Oliver Lange, David van der Spoel, and Bert L de Groot

Supplement: Scrutinizing Molecular Mechanics Force Fields on the Microsecond Timescale with NMR Data

Oliver F. Lange[1], David van der Spoel[2], Bert L. de Groot[3#]

Affiliation 1:
Department of Biochemistry
University of Washington
Seattle, WA 98195, USA

Affiliation 2:
Dept. of Cell & Molecular Biology
Uppsala University
Box 596, 75124 Uppsala, Sweden

Affiliation 3:
Department of Theoretical and Computational Biophysics
Max-Planck-Institute for Biophysical Chemistry
Am Fassberg 11, 37077 Göttingen, Germany
[#]Corresponding author: Bert de Groot

Department of Theoretical and Computational Biophysics
Max-Planck-Institute for Biophysical Chemistry
Am Fassberg 11, 37077 Göttingen, Germany
Phone: +49-551-201-2308, Fax: +49-551-201-2302
Email: bgroot@gwdg.de

Keywords: molecular dynamics, ensemble, consensus, nuclear magnetic resonance, residual dipolar couplings, hydrogen bonds, force-field validation

1. METHODS

1.1. **Molecular Dynamics Simulations.** All MD simulations were carried out using the GROMACS simulation package[1, 2] in explicit solvent and periodic boundary conditions. Starting coordinates were obtained from pdb entries 1ubq and 2igd, for the proteins ubiquitin and gb3, respectively. A truncated dodecahedral simulation box was chosen such that the water layer separating two periodic images of the protein was at least 2 nm. All simulations were carried out using physiological salt concentrations by applying 150 mM NaCl. Starting configurations were energy minimized using the steepest descent algorithm. Prior to the production runs, equilibration simulations with a length of 1 ns were carried out with position restraints (k=1000 kJ $mol^{-1}nm^{-2}$) on the protein heavy atoms. The temperature was kept constant at 300K by coupling the system (τ= 0.1 ps) to a temperature bath[3]. Likewise, the pressure was kept constant at 1 bar by coupling the system (τ= 1 ps) to a pressure bath[3]. The following all-atom force fields were used: opls/aa-l[4], amber99sb[5] and amber03[6, 7], charmm-22[8], gromos96-43a1 and gromos96-53a6[9]. Simulation parameters were chosen to closely match the setup in which the force field parameters were developed, respectively. For the gromos96 simulations marked "cutoff" a reaction field with $\epsilon = 54$ was applied beyond a cutoff of 14 Å, for the opls/aa "cutoff" simulations a straight cut-off of 14 Å was chosen, and for the charmm "cutoff" simulations a shift function was used between 10 and 12 Å. In addition, simulations were carried out using Particle Mesh Ewald (PME) for the calculation of electrostatic interactions[10, 11]. Cut-off radii for van der Waals interactions were set to 14 Å, except for the simulations using the charmm force field, where a shift function was used between 10 and 12 Å. In the g96 simulations the SPC water model[12] was applied. For the simulations carried out in the charmm-22, amber99sb and amber03 force fields, TIP3P[13] was used as water model. The opls/aa simulations were carried out using TIP4P[13] as water model. Lincs[14] was used to constrain bond-lengths, allowing a time step of 2 fs. Structures were stored every 1 ns and superimposed via least squares fit of their backbone atoms to the crystal structure 1ubq and 2igd, respectively. Flexible tails (residues 71-76 and residues 1-5 for ubiquitin and gb3, respectively) were excluded from this fit.

1.2. **Computation of residual dipolar couplings.** Residual dipolar couplings were computed from the least squares fitted MD ensembles with snapshots every 1 ns, obtained as described above. For each interaction vector of interest $\mathbf{r}^i_{XY}(t) = \mathbf{x}(X_i) - \mathbf{x}(Y_{f(i)})$ and (θ_t, φ_t) denoting its spherical coordinates, we obtain ensemble averaged 2nd rank spherical harmonics $s^i_m(X,Y) = \langle Y_{2m}(\theta_t, \varphi_t)\rangle_t$, with $m = -2...2$. Here $\mathbf{x}(X_i)$ denotes the position of atom X in residue i and $\mathbf{x}(Y_{f(i)})$ the position of a coupled nucleus with $f(i) = i$ for atom-pairs XY $=NH$, $C_\alpha H$ and $f(i) = i + 1$ for atom-pairs CH, CN, CC_α. The ensemble average $<>_t$ comprises either the snapshots of the entire MD trajectory or snapshots falling into a particular window of shorter length. The residual dipolar coupling of atom-pair $X_i, Y_{f(i)}$ in alignment medium $n \in 1, ..., N$ is given as

$$\delta^i_{XY}(n) = \eta_{XY} \left\| \left\langle \mathbf{r}^i_{XY} \right\rangle \right\|^{-3} \sum_{m=-2...2} s^i_m(X,Y) t^n_m, \tag{1.1}$$

where t^n_m denotes the alignment tensor[15]. For each alignment medium n usually a large ($\gg 5$) number of couplings are available, and the five parameters t^n_m are obtained by singular value decomposition of the over determined system of equations (Eq. 1.1)[16].

The residual dipolar coupling data used for ubiquitin has been taken from Ref. [17] and for gb3 from Ref. [18]. The amount of data available for the various atom-pairs varies greatly. Supplement Figure S1 shows, however, that the particular selection of certain sets of atom-pairs doesn't change the conclusion, i.e., the relative differences between force fields. We carried out all subsequent analyses on atom-pairs NH,CH, and NC, for which a reasonable number of couplings are available for both proteins.

R-values were computed individually,

$$R_{\mathrm{X}} = \left(\Sigma_k^{n_x} \left(\mathrm{X_{k,calc}} - \mathrm{X_{k,exp}} \right)^2 / \left(2 \sum_k^{n_x} \mathrm{X_{k,exp}^2} \right) \right)^{1/2},$$

for every data class X with n_{x} data points and subsequently averaged[19]. Here, a data-class comprises all couplings between the same types of nuclei determined in the same alignment medium.

2. Results

2.1. **Molecular Surface.** We computed the solvent accessible surface with a spherical probe of radius 0.14nm for all MD snapshots. The surface areas generated by the various force-fields are more consistent with each other than the other observables discussed in the main text. However, as shown in supplement Figure S11 some systematic outliers can be found. As one extreme, structures generated with the g96_43a1 force-field have a significantly smaller molecular surface for both proteins. The opposite is the case for force-fields charmm22 and opls/aa if combined with cutoff electrostatics which have a strong tendency towards structures with larger molecular surfaces.

References

[1] Hess, B.; Scheek, R. M. *J. Magn. Res.* **2003**, *164*(1), 19–27.
[2] van der Spoel, D.; van Maaren, P. J. *J. Chem. Theory Comput.* **2005**, *2*(1), 1–11.
[3] Berendsen, H. J. C.; Postma, J. P. M.; DiNola, A.; Haak, J. R. *J. Chem. Phys.* **1984**, *81*, 3684–3690.
[4] Jorgensen, W. L.; Maxwell, D. S.; Tirado-Rives, J. *J. Am. Chem. Soc.* **1996**, *118*, 11225–11236.
[5] Hornak, V.; Abel, R.; Okur, A.; Strockbine, B.; Roitberg, A.; Simmerling, C. *Proteins: Structure, Function, and Bioinformatics* **2006**, *65*(3), 712–725.
[6] Duan, Y.; Wu, C.; Chowdhury, S.; Lee, M. C.; Xiong, G. M.; Zhang, W.; Yang, R.; Cieplak, P.; Luo, R.; Lee, T.; Caldwell, J.; Wang, J. M.; Kollman, P. *J. Comput. Chem.* **2003**, *24*(16), 1999–2012.
[7] Sorin, E. J.; Pande, V. S. *Biophys. J.* **2005**, *88*(4), 2472–2493.
[8] MacKerell, A. D.; Bashford, D.; Bellott, M.; Dunbrack, R. L.; Evanseck, J. D.; Field, M. J.; Fischer, S.; Gao, J.; Guo, H.; Ha, S.; Joseph-McCarthy, D.; Kuchnir, L.; Kuczera, K.; Lau, F. T. K.; Mattos, C.; Michnick, S.; Ngo, T.; Nguyen, D. T.; Prodhom, B.; Reiher, W. E.; Roux, B.; Schlenkrich, M.; Smith, J. C.; Stote, R.; Straub, J.; Watanabe, M.; Wiorkiewicz-Kuczera, J.; Yin, D.; Karplus, M. *J. Phys. Chem. B* **1998**, *102*(18), 3586–3616.
[9] Oostenbrink, C.; Villa, A.; Mark, A. E.; Gunsteren, W. F. V. *J. Comput. Chem.* **2004**, *25*(13), 1656–1676.
[10] Essmann, U.; Perera, L.; Berkowitz, M. L.; Darden, T.; Lee, H.; Pedersen, L. G. *J. Chem. Phys.* **1995**, *103*(19), 8577–8593.
[11] Darden, T.; York, D.; Pedersen, L. *J. Chem. Phys.* **1993**, *98*, 10089–10092.
[12] Berendsen, H. J. C.; Postma, J. P. M.; van Gunsteren, W. F.; Hermans, J. In *Intermolecular Forces*; Pullman, B., Ed.; D. Reidel Publishing Company: Dordrecht, 1981; pages 331–342.
[13] Jorgensen, W. L.; Chandrasekhar, J.; Madura, J. D.; Impey, R. W.; Klein, M. L. *J. Chem. Phys.* **1983**, *79*, 926–935.
[14] Hess, B.; Bekker, H.; Berendsen, H. J. C.; Fraaije, J. G. E. M. *J. Comput. Chem.* **1997**, *18*, 1463–1472.
[15] Tolman, J. R.; Ruan, K. *Chem. Rev.* **2006**, *106*(5), 1720–1736.
[16] Losonczi, J. A.; Andrec, M.; Fischer, M. W. F.; Prestegard, J. H. *J. Mag. Res.* **1999**, *138*, 334–342.

[17] Lakomek, N.-A.; Walter, K. F. A.; Fares, C.; Lange, O. F.; de Groot, B. L.; Grubmueller, H.; Brueschweiler, R.; Munk, A.; Becker, S.; Meiler, J.; Griesinger, C. Jan **2008**, *41*(3), 139–155.

[18] Bouvignies, G.; Markwick, P.; Bruschweiler, R.; Blackledge, M. *J. Am. Chem. Soc.* **2006**, *128*(47), 15100–15101.

[19] Lange, O. F.; Lakomek, N.-A.; Fares, C.; Schroeder, G. F.; Walter, K. F. A.; Becker, S.; Meiler, J.; Grubmueller, H.; Griesinger, C.; de Groot, B. L. Jan **2008**, *320*(5882), 1471–1475.

[20] Cornilescu, G.; Hu, J.-S.; Bax, A. *J. Am. Chem. Soc.* **1999**, *121*(12), 2949–2950.

[21] Cordier, F.; Grzesiek, S. *J. Am. Chem. Soc.* **1999**, *121*(7), 1601–1602.

[22] Lange, O. F.; Lakomek, N.-A.; Fares, C.; Schröder, G. F.; Walter, K. F. A.; Becker, S.; Meiler, J.; Grubmüller, H.; Griesinger, C.; de Groot, B. L. *Science* **2008**, *320*(5882), 1471–1475.

[23] Salmon, L.; Bouvignies, G.; Markwick, P.; Lakomek, N.; Showalter, S.; Li, D.-W.; Walter, K.; Griesinger, C.; Brueschweiler, R.; Blackledge, M. Jan **2009**, *48*(23), 4154–4157.

[24] Markwick, P. R. L.; Bouvignies, G.; Salmon, L.; McCammon, J. A.; Nilges, M.; Blackledge, M. Jan **2009**, *131*(46), 16968–16975.

TABLE S1. At the end of the supplement we attached tables with deviation from experimental[20, 21] ^{3h}J couplings across hydrogen bonds in the various simulation protocols for ubiquitin and gb3.

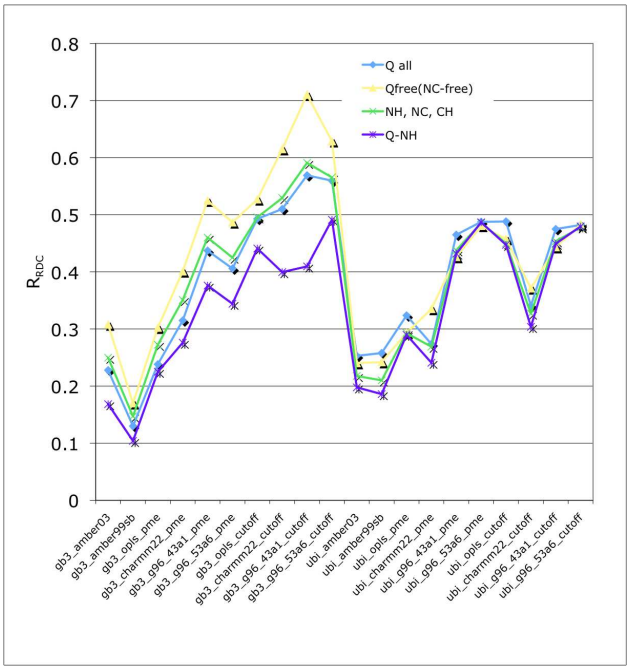

FIGURE S1. Comparison of R_{RDC} computed for different combinations of nuclei. All dipolar couplings present in the data set (blue) are NH, NC, CH, CaC, CaCb and side-chain methyl groups. In Ref. [22] the free R_{RDC} was computed over the NC couplings after fitting of the alignment tensor via all couplings except the NC. This particular value is computed here for all MD trajectories (yellow). R_{RDC} computed over all NH, NC, and CH couplings(green). R_{RDC} computed over NH-couplings, only (purple).

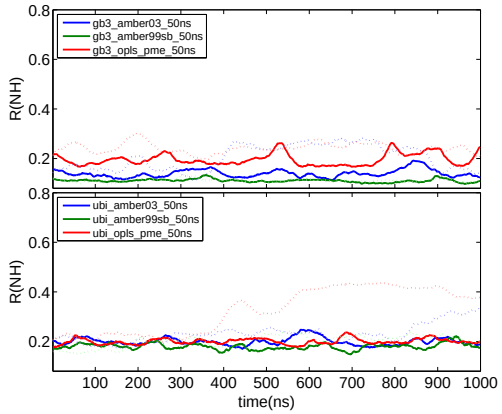

FIGURE S2. Time resolved R_{RDC} for MD simulations in selected force-fields that are "reset" every 50ns. For comparison, the corresponding full-length $1\,\mu s$ trajectories are plotted as dotted lines in the same color with less intensity.

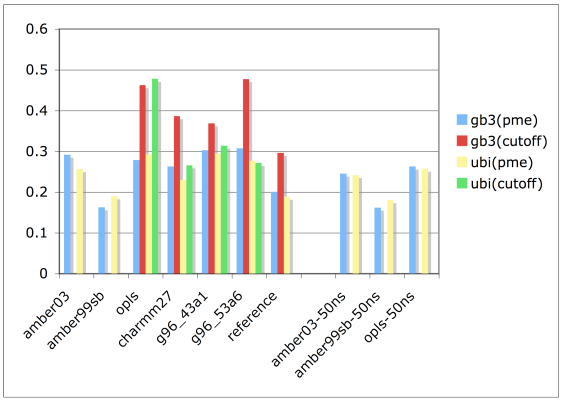

FIGURE S3. Overview of analysis of ${}^{3h}J_{\mathrm{NC}}$ across hydrogen bond couplings. The bar plot shows $R^{1000}_{\mathrm{h-bond}}$ for various force-fields and simulation protocols for protein gb3 and ubiquitin. The values labelled as "reference" is 2igd (blue) and 1igd (red) for gb3 and 2k39 (yellow) for ubiquitin, respectively.

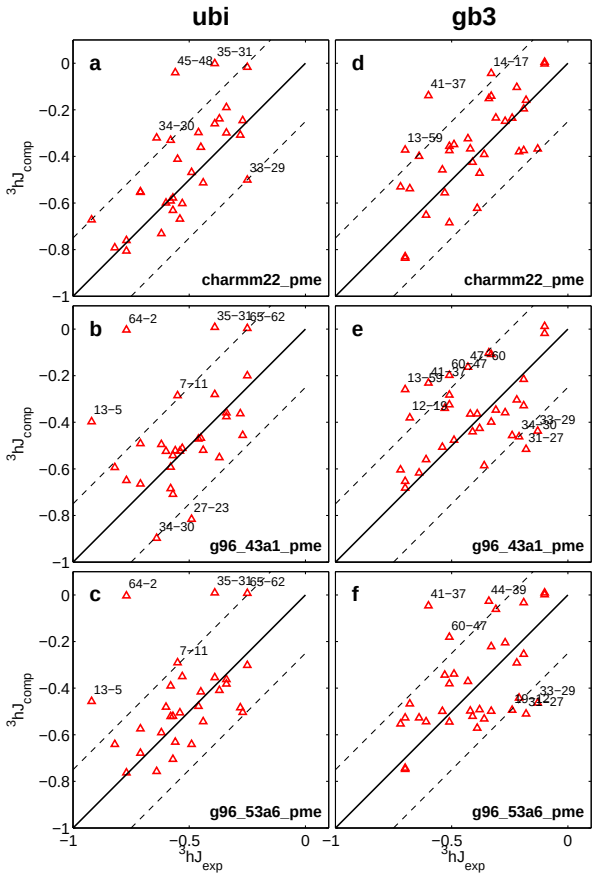

FIGURE S4. Comparison of $^{3h}J_{exp}$ couplings accross hydrogen bonds for proteins ubiquitin (left) and gb3 (right) with couplings backcalculated from MD simulations carried out with force-fields charmm22 (a,d), g96_43a1 (b,e) and g96_53a6 (c,f). The same plot for the remaining simulations is shown in main-text Figure 4.

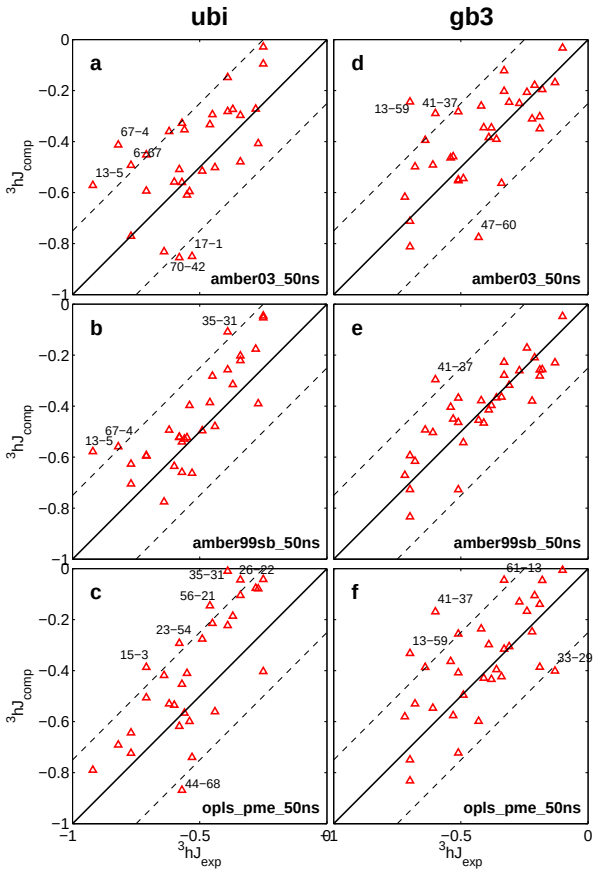

FIGURE S5. Comparison of ${}^{3h}J_{exp}$ couplings accross hydrogen bonds for proteins ubiquitin (left) and gb3 (right) with couplings backcalculated from MD simulations carried out with force-fields amber03 (a,d), amber99sb (b,e) and opls/aa (c,f) that were restarted from an equilibrated crystal structure every 50 ns.

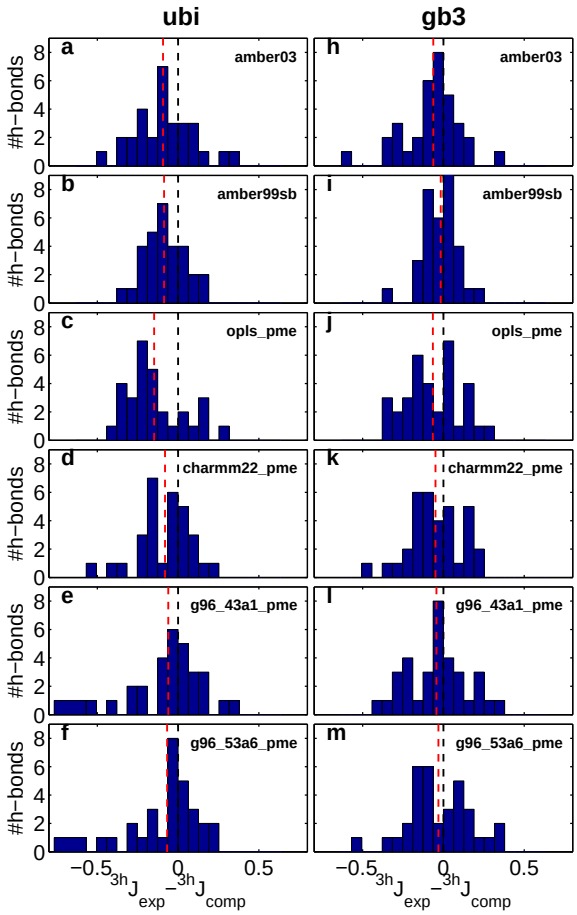

FIGURE S6. Histogram of prediction differences for ${}^{3h}J$ couplings across hydrogen bonds. The black dashed line marks a difference of $0\,\mathrm{Hz}$. The red dashed line is the mean prediction difference of the shown distribution.

‘

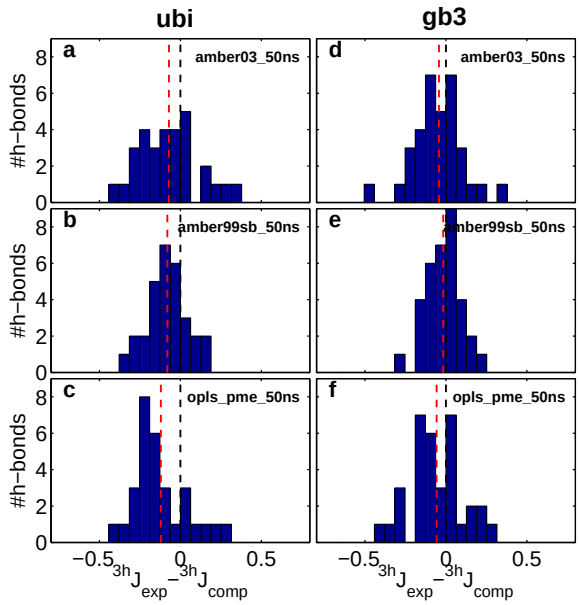

FIGURE S7. Histogram of prediction errors for ${}^{3h}J$ couplings across hydrogen bonds similar to Figure S6 but computed from 20 $50\,\mathrm{ns}$ MD trajectories rather than a single $1000\,\mathrm{ns}$ trajectory.

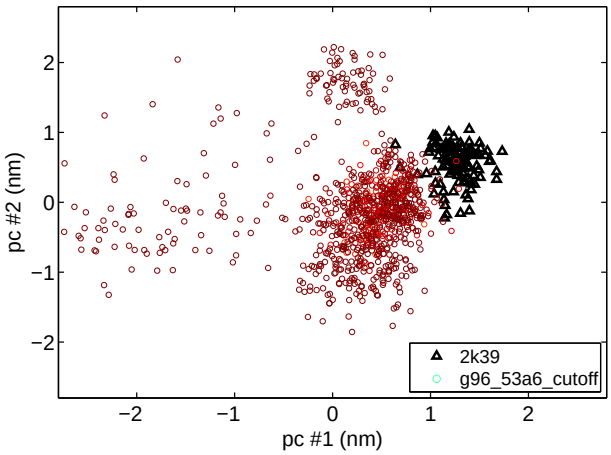

FIGURE S8. Principal component analysis (PCA) of the MD simulation of ubiquitin with force-field g96_53a6 and cutoff electrostatics (this plot complements the panels in Fig. 6 of the main text). PCA is carried out over the combined set of structures taken from the 2k39 (black) ensemble and the g96_53a6 (colored) ensemble. The coloring is consistent with that of Fig. 6 with blue for the lowest R^{50}_{RDC}values and red for the highest R^{50}_{RDC}-values.

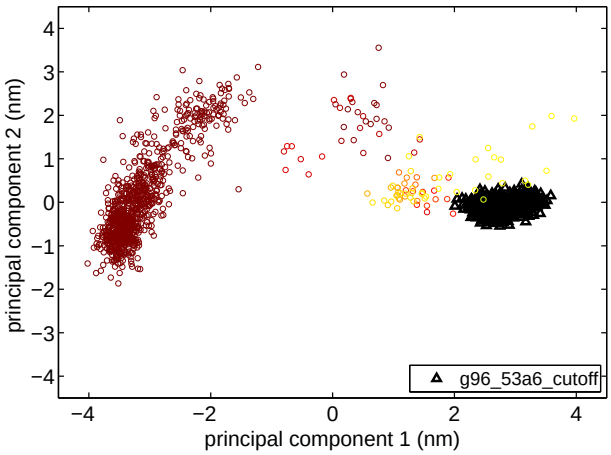

FIGURE S9. Principal component analysis (PCA) of the MD simulation of gb3 with g96_53a6 with cutoff electrostatics (this plot complements the panels in Fig. 7). PCA is carried out over the combined set of structures taken from the amber99sb (black) ensemble and the g96_53a6 (colored) ensemble. The coloring is consistent with that of Fig. 7 with blue for the lowest R^{50}_{RDC} values and red for the highest R^{50}_{RDC}-values.

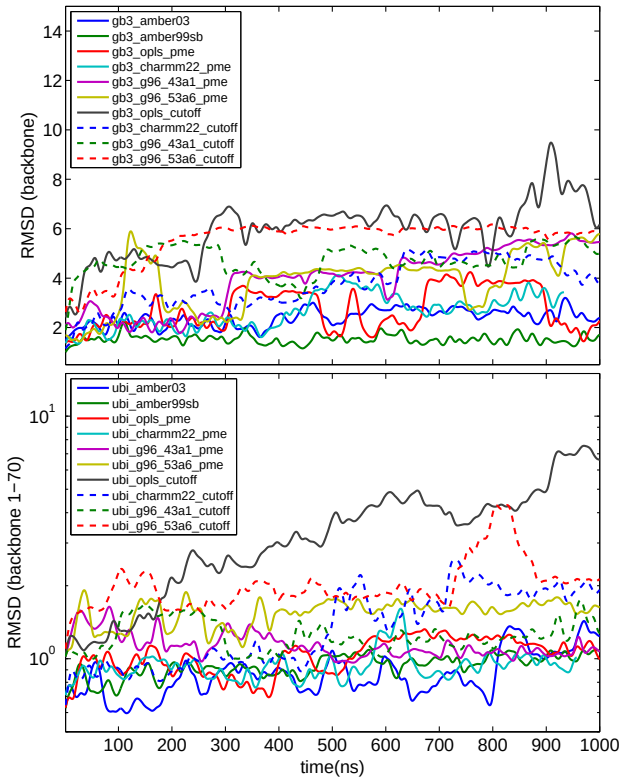

FIGURE S10. Root mean square deviation (RMSD) in Angstrom against (apo) X-ray structure for MD structures generated by various force-fields.

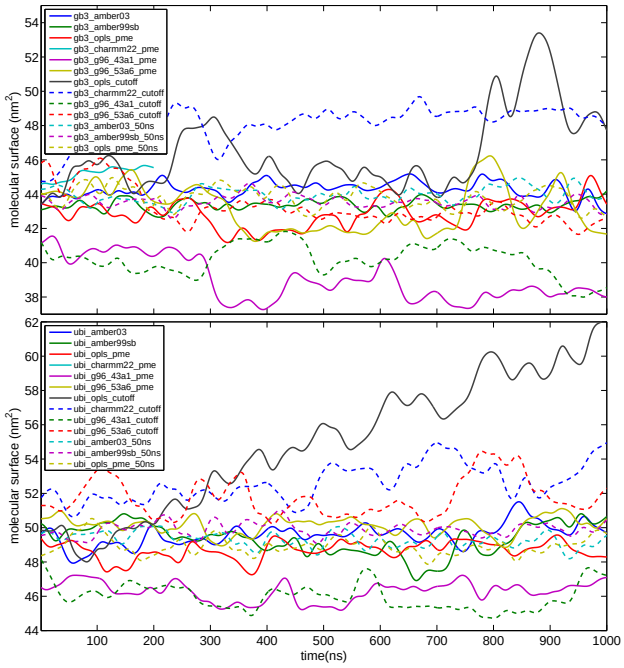

FIGURE S11. Total solvent accessible surface area during MD simulations of gb3 and ubiquitin (time averaged).

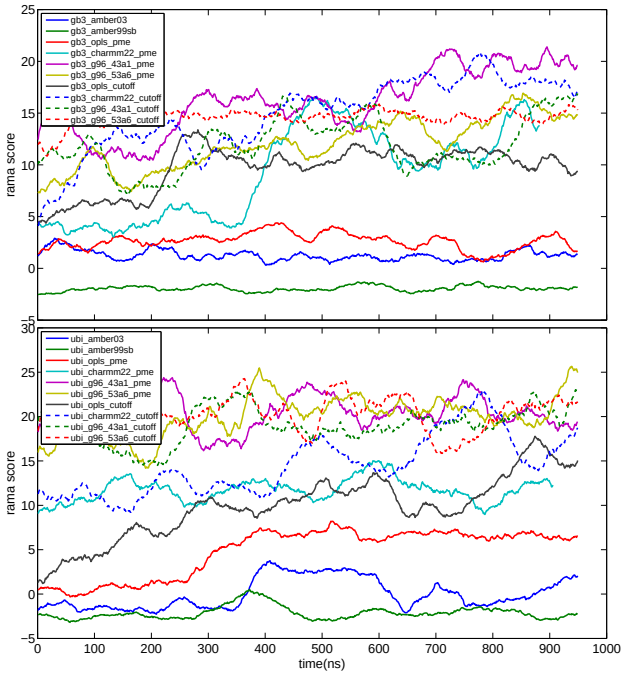

FIGURE S12. Quality of backbone torsions during the time course of the MD simulations. The backbone torsion quality score shown here is a running average (50ns) of the 'rama' ROSETTA energy term, which is based on the compatibility of backbone torsions at each residue with the aminoacid-type dependent ramachandran plot.

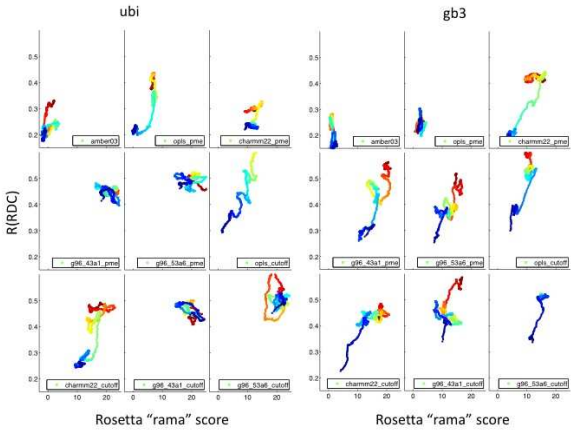

FIGURE S13. The quality of predicted RDCs compared directly to quality of predicted ${}^{3h}J$ couplings across hydrogen bonds. The simulation time is color coded from blue ($0.0\,\mu s$) to red ($1.0\,\mu s$) .

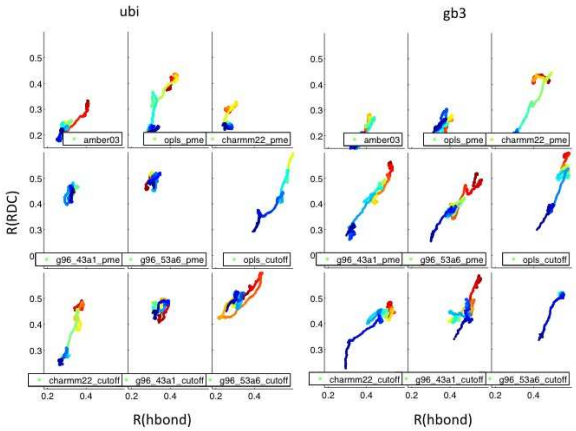

FIGURE S14. The quality of predicted RDCs compared directly to quality of predicted ${}^{3h}J$ couplings across hydorgen bonds. The simulation time is color coded from blue ($0.0\,\mu s$) to red ($1.0\,\mu s$) .

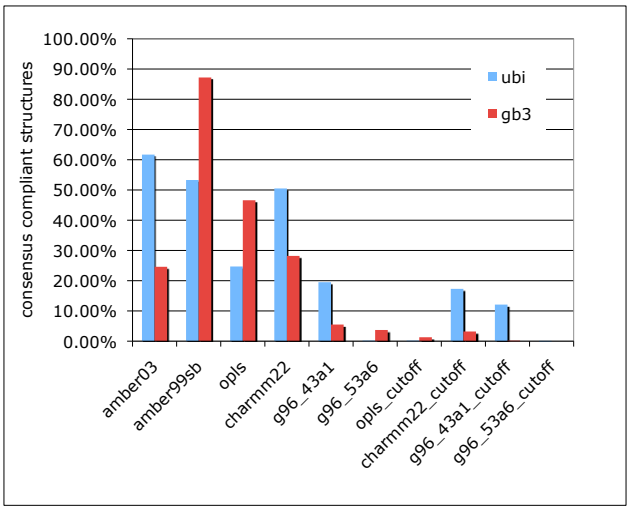

FIGURE S15. Contributions of different force-fields to the RMSD selected consensus ensembles. The first 6 are with PME electrostatics, whereas the last 4 are cutoff or reaction field (labelled uniformly as cutoff). ($N_{\text{sel}} = 6$, $M_{\text{match}} = 1$)

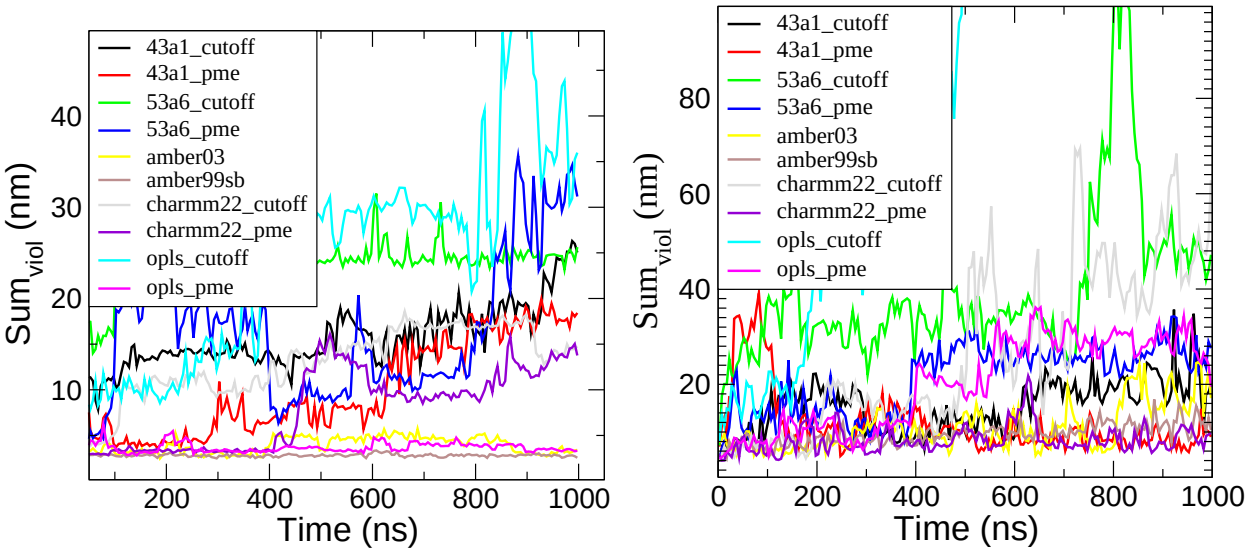

(A) NOE violations for gb3

(B) NOE violations for ubi

FIGURE S16. Time resolved NOE violations for MD simulations carried out with various force-fields

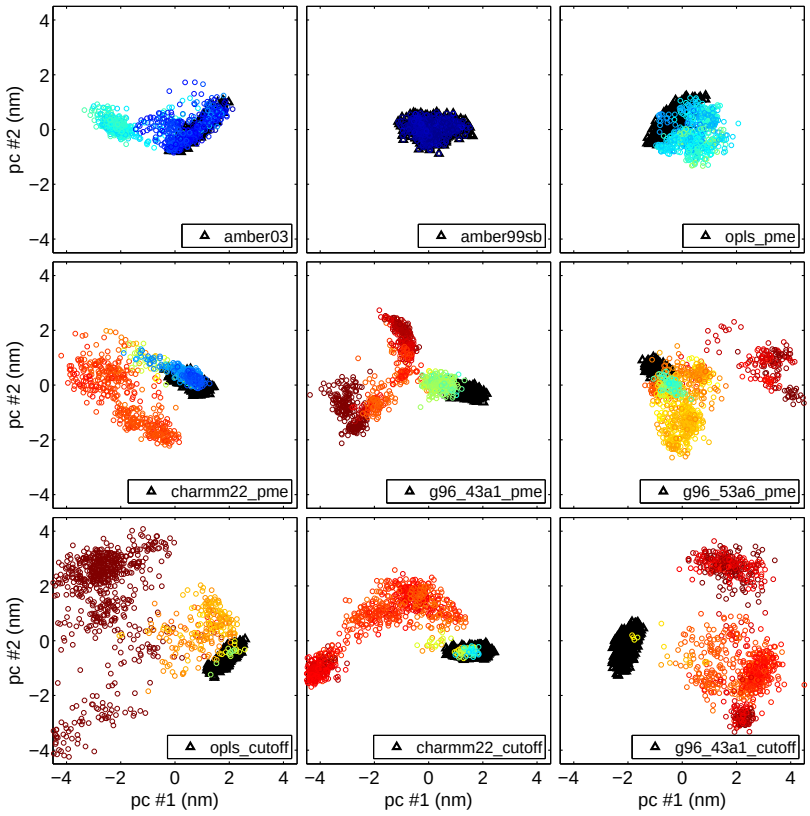

FIGURE S17. Principal component analysis (PCA) of gb3 ensembles. For each panel, PCA is carried out over the combined set of structures taken from a reference ensemble and the respective force-field ensemble. Unlike for ubiquitin for this protein no suitable reference ensemble exists. We therefore selected the amber99sb ensemble as reference. The coloring depicts the 50ns-window average of R_{RDC} for a given snapshot (cf. Fig 3), all panels use the same color-scale as in Fig. 5 with blue for the lowest R_{RDC}-values and red for the highest R_{RDC}-values. The first principal component (x-axis) contributes >30% to the overall motion for all trajectories with the exceptions of amber03, amber99sb, charmm22_pme and g96_43a1_pme, where it contributes 20%, 19%, 15% and 19%, respectively.

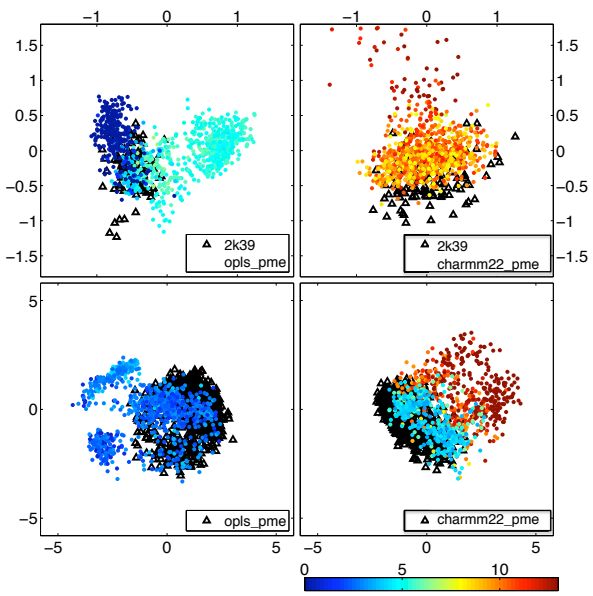

FIGURE S18. Relation between conformation and Ramachandran "rama" score for selected MD ensembles. Snapshots are projected into the xy-plane according to the first two principal components as shown in Fig. 5 and Fig. S18. The color codes the ROSETTA rama score term. The upper panels refer to ubiquitin, the lower panels to gb3.

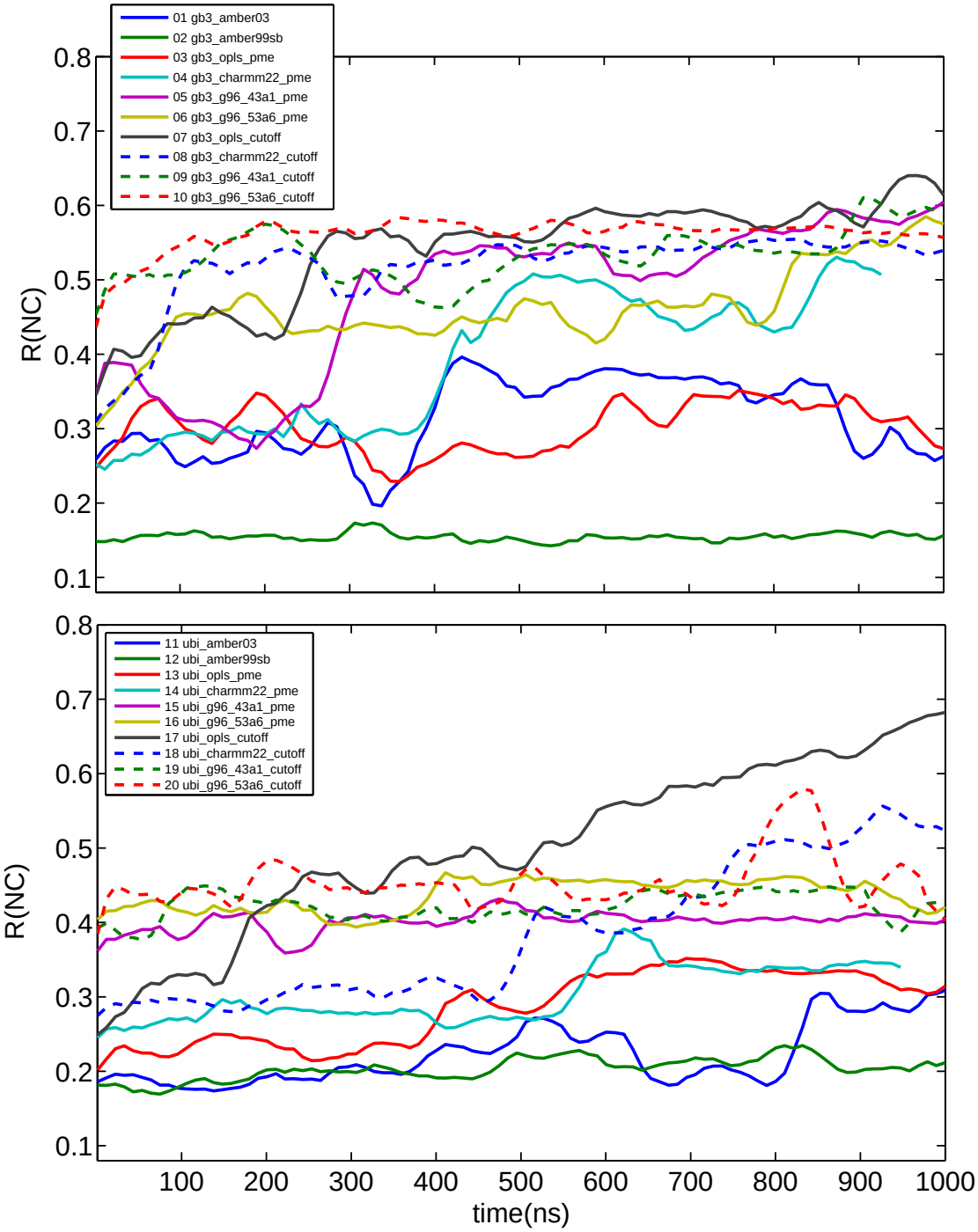

FIGURE S19. Time resolved $NC - R_{\mathrm{RDC}}$ for MD simulations with various force-fields. The residual dipolar couplings were computed from the respective MD trajectory in (overlapping) windows of 50 ns length.

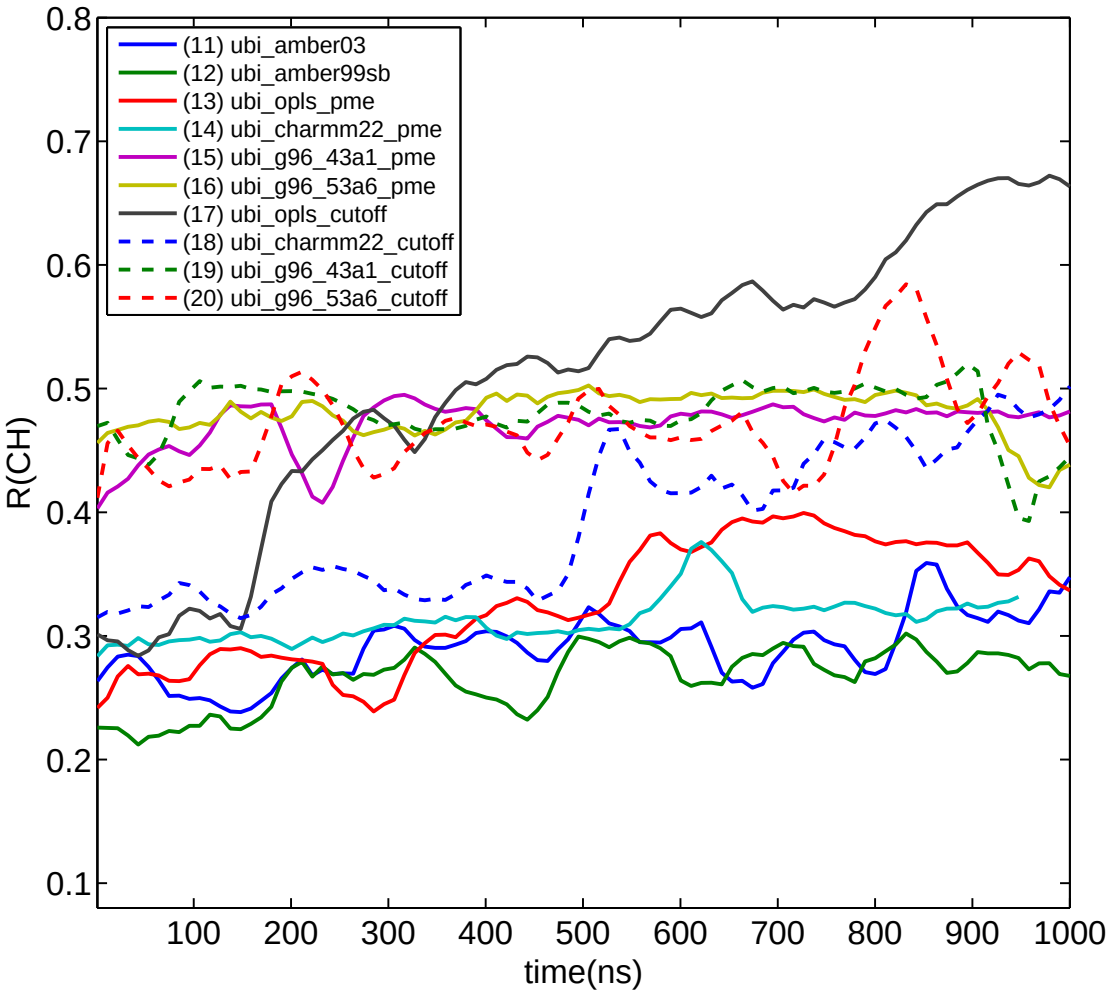

FIGURE S20. Time resolved $CH - R_{\mathrm{RDC}}$ for MD simulations with various force-fields. The residual dipolar couplings were computed from the respective MD trajectory in (overlapping) windows of 50 ns length.

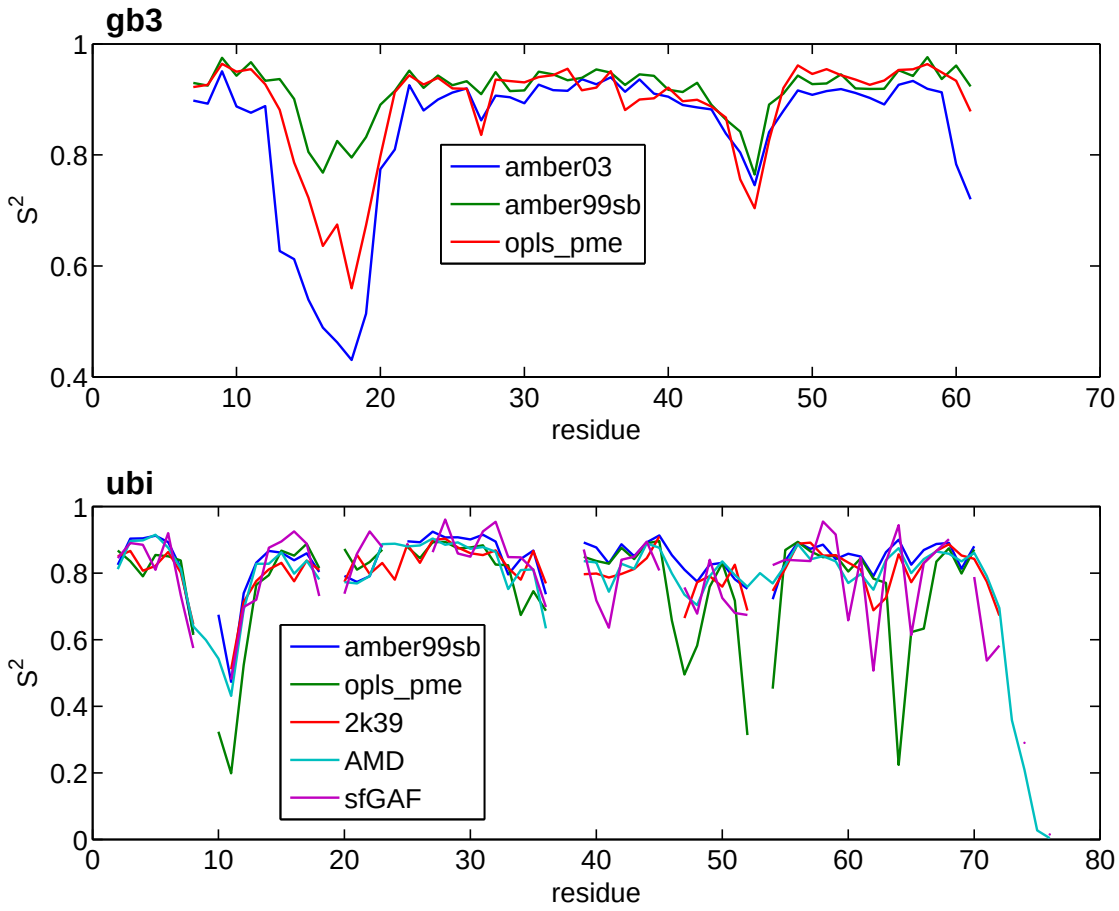

FIGURE S21. Order parameter (S^2) computed for N-H bonds from ensembles (amber03/amber99sb/opls/2k39/amd) and directly from the RDC data with the structure-free GAF-Analysis (sfGAF) reported in Ref. [23]. The S^2 order parameters from the accelerated molecular dynamics ensemble (AMD) were taken directly from Ref. [24].

Hydrogen bond	Amber03	Amber99sb	Opls/aa	Charmm27	G96_43a1	G96_53a6
3 - 15	0.0874	0.0654	0.1453	0.0731	0.0798	0.1032
4 - 65	-0.1197	0.0256	-0.2987	-0.0006	-0.0759	-0.1191
6 - 67	-0.3208	-0.1175	-0.2098	-0.0095	-0.1208	-0.0067
7 - 11	0.0199	0.0156	-0.3577	-0.1386	-0.2648	-0.2596
13 - 5	-0.3546	-0.3652	-0.221	-0.248	-0.5226	-0.4633
15 - 3	-0.1181	-0.1081	-0.3539	-0.1562	-0.2188	-0.1357
17 - 1	0.3242	0.1718	0.1398	0.0721	-0.0187	-0.1802
23 - 54	-0.188	-0.1331	-0.3551	-0.2496	0.1043	-0.1898
26 - 22	0.0714	-0.1969	-0.296	-0.1502	0.0189	0.0227
27 - 23	0.0096	0.0099	-0.2518	-0.0219	0.3259	0.1508
28 - 24	-0.0333	-0.0955	-0.176	0.0281	0.0827	0.2037
29 - 25	0.1027	0.1088	-0.1548	-0.0244	0.186	0.2335
30 - 26	-0.0973	-0.0388	-0.1608	-0.1318	0.1811	0.0392
31 - 27	-0.1583	-0.1498	-0.2089	-0.0895	0.018	-0.0343
32 - 28	-0.0555	-0.1406	-0.2065	-0.0413	0.0353	0.042
33 - 29	-0.213	-0.1989	0.1725	0.2509	-0.0501	0.0519
34 - 30	0.155	0.1279	-0.2446	-0.3198	0.2574	0.117
35 - 31	-0.2591	-0.271	-0.3824	-0.3889	-0.3979	-0.3994
42 - 70	-0.2327	-0.1058	0.0516	0.0078	-0.0274	-0.0496
44 - 68	-0.036	0.0399	0.2575	0.0611	0.1388	0.135
45 - 48	-0.2845	-0.0307	0.074	-0.5199	-0.0385	0.0712
50 - 43	-0.2459	-0.117	-0.0817	-0.1588	-0.0458	-0.0315
56 - 21	-0.0945	-0.1077	-0.2299	-0.1626	0.0113	0.0175
57 - 19	-0.1176	-0.1172	-0.1357	-0.1306	-0.1096	-0.0357
64 - 2	-0.1112	-0.0626	-0.3782	0.0356	-0.7664	-0.7665
65 - 62	-0.1242	-0.2077	-0.1877	-0.2329	-0.2534	-0.2573
67 - 4	-0.4813	-0.2503	-0.2791	-0.0283	-0.2263	-0.1789
68 - 44	-0.2354	-0.1453	-0.0828	0.1108	-0.125	-0.0295
69 - 6	0.032	-0.1776	0.0024	0.1283	-0.0166	-0.0344
70 - 42	0.2841	-0.0357	-0.0315	0.0106	0.012	-0.0589

Caption: Deviation of J-coupling across hydrogen bond (J_{exp}-J_{comp}) backcalculated from PME trajectories of ubiquitin

Hydrogen bond	Opls/aa	Charmm27	G96_43a1	G96_53a6
3 - 15	0.2017	0.1395	0.122	0.1301
4 - 65	-0.6078	-0.0666	-0.0968	-0.2206
6 - 67	-0.1793	-0.0445	-0.1052	0.04
7 - 11	-0.4687	-0.1162	-0.3706	-0.2604
13 - 5	-0.6162	-0.2544	-0.5102	-0.357
15 - 3	-0.2681	-0.1039	-0.1878	-0.1193
17 - 1	0.1592	0.0872	-0.1489	-0.2575
23 - 54	-0.5157	-0.212	0.1788	-0.0006
26 - 22	-0.3209	-0.1711	0.0283	0.0501
27 - 23	-0.2806	0.007	0.3438	0.1921
28 - 24	-0.1926	0.0499	0.1792	0.1939
29 - 25	-0.2644	-0.033	0.1909	0.208
30 - 26	-0.2391	-0.1237	0.1642	-0.0505
31 - 27	-0.1979	-0.1056	-0.005	-0.0973
32 - 28	-0.3109	0.0192	-0.031	-0.1185
33 - 29	-0.1478	0.2727	-0.0485	0.017
34 - 30	-0.5318	-0.3932	0.1217	-0.1503
35 - 31	-0.396	-0.3744	-0.3976	-0.3923
42 - 70	-0.34	-0.3439	-0.2431	-0.1651
44 - 68	0.1141	0.0745	0.2198	0.1814
45 - 48	-0.3786	-0.482	-0.0677	-0.043
50 - 43	-0.617	-0.1883	-0.0608	-0.137
56 - 21	-0.0716	-0.1624	0.0666	0.0712
57 - 19	-0.2417	-0.1227	-0.0979	-0.0739
64 - 2	-0.7795	-0.4168	-0.7781	-0.7167
65 - 62	-0.1794	-0.2478	-0.2464	-0.223
67 - 4	-0.6435	-0.0386	-0.2281	-0.1712
68 - 44	-0.201	0.0453	-0.1241	-0.0305
69 - 6	-0.0322	0.1427	-0.2021	0.0012
70 - 42	-0.2156	-0.1113	0.0053	0.0237

Caption: Deviation of J-coupling across hydrogen bond (J_{exp}-J_{comp}) backcalculated from cutoff or reaction field trajectories of ubiquitin

Hydrogen bond	Amber03	Amber99sb	Opls/aa	Charmm27	G96_43a1	G96_53a6
8 - 23	0.0973	0.215	0.1965	0.1742	-0.1858	0.0349
9 - 55	-0.1498	-0.0485	-0.1753	-0.0527	-0.0559	0.0774
10 - 21	-0.057	0.1091	0.0365	0.1363	-0.0468	0.0481
12 - 19	-0.3307	-0.0722	-0.16	-0.1419	-0.2992	-0.2131
13 - 59	-0.6129	-0.0702	-0.3776	-0.3281	-0.4406	-0.1727
14 - 17	-0.1086	-0.0364	0.0501	-0.2866	0.0686	0.1687
19 - 12	0.0477	-0.0768	-0.0837	-0.0046	0.2166	0.254
21 - 10	0.1542	0.0288	0.0358	0.0915	0.0456	0.112
23 - 8	-0.0932	0.0624	-0.021	0.0147	0.0303	0.1105
25 - 6	-0.0118	-0.0534	-0.1632	-0.1352	-0.2272	-0.1295
31 - 27	-0.0024	0.0597	-0.1328	-0.0213	0.3357	0.3303
32 - 28	-0.0907	-0.1229	-0.2355	-0.0828	-0.0334	-0.041
33 - 29	0.055	0.0916	0.272	0.2377	0.3075	0.3332
34 - 30	-0.0371	-0.0159	-0.1169	0.1695	0.2518	0.2318
35 - 31	-0.2904	-0.1482	-0.2833	-0.2409	-0.023	-0.1127
36 - 32	-0.1195	-0.0704	-0.1989	-0.1899	-0.116	-0.1671
37 - 33	0.098	0.1185	-0.1153	0.1842	0.0252	0.0641
38 - 34	-0.0168	-0.0027	-0.198	-0.0212	0.0886	-0.0653
39 - 35	0.0629	0.0356	0.0221	-0.1413	-0.0135	-0.151
40 - 36	-0.0373	0.0157	0.0503	-0.0753	0.0371	-0.2486
41 - 37	-0.33	-0.3195	-0.3523	-0.4613	-0.3689	-0.5536
42 - 38	0.1208	0.0792	0.1715	0.0053	0.1384	-0.1571
43 - 40	-0.0634	-0.0546	-0.0922	-0.0971	-0.0817	-0.1013
44 - 39	0.157	0.0183	0.1828	-0.1889	-0.239	-0.3135
47 - 60	0.3314	0.0532	0.1448	-0.1063	-0.2669	-0.0592
49 - 58	-0.0112	-0.0826	0.0675	0.0257	-0.1904	-0.1866
51 - 56	0.0624	0.0199	0.044	0.0311	0.226	0.1718
54 - 51	-0.1352	-0.1506	-0.1335	-0.1049	-0.112	-0.1094
56 - 51	0.0578	0.1622	0.0087	-0.1166	0.0837	0.0713
57 - 9	-0.03	0.0017	0.1437	0.1299	-0.0179	0.043
58 - 49	-0.1157	-0.105	-0.0514	0.0417	-0.05	-0.0662
59 - 11	-0.2569	0.0281	-0.158	0.2324	-0.0262	0.1813
60 - 47	-0.2162	-0.1379	-0.279	-0.1537	-0.3119	-0.3291
61 - 13	-0.2683	-0.1123	-0.3193	-0.1891	-0.2218	-0.1084

Caption: Deviation of J-coupling across hydrogen bond (J_{exp}-J_{comp}) backcalculated from PME trajectories of GB3

Hydrogen bond	Opls/aa	Charmm27	G96_43a1	G96_53a6
8 - 23	0.1166	0.207	-0.4012	0.1039
9 - 55	-0.2564	0.0357	-0.2672	0.2748
10 - 21	-0.2644	0.1536	-0.1524	-0.1518
12 - 19	-0.2472	-0.3269	-0.3166	-0.1437
13 - 59	-0.5079	-0.606	-0.4413	-0.6911
14 - 17	-0.0562	-0.162	0.0363	0.4237
19 - 12	0.1448	-0.0547	0.1585	0.3822
21 - 10	0.2692	0.1245	0.0599	0.135
23 - 8	0.1038	-0.0038	-0.0333	0.1364
25 - 6	-0.2603	-0.1143	-0.4095	-0.1134
31 - 27	-0.0773	0.0627	0.2537	0.1601
32 - 28	-0.481	-0.1096	-0.1282	-0.2369
33 - 29	-0.0321	0.1182	0.2185	-0.0777
34 - 30	-0.0437	0.2328	0.3869	-0.1659
35 - 31	-0.5856	-0.3194	-0.0576	-0.6154
36 - 32	-0.6307	-0.3282	-0.2739	-0.6592
37 - 33	-0.1056	0.3289	0.3166	-0.1561
38 - 34	-0.2622	-0.0821	0.3068	-0.2501
39 - 35	-0.3841	-0.3856	-0.0688	-0.4652
40 - 36	-0.2031	-0.2486	-0.1517	-0.3077
41 - 37	-0.5949	-0.5663	-0.3542	-0.5963
42 - 38	-0.1775	-0.1371	-0.1684	-0.1869
43 - 40	-0.1051	-0.099	-0.0995	-0.1002
44 - 39	-0.3288	-0.3116	-0.3306	-0.3382
47 - 60	-0.4134	-0.3438	-0.0578	0.0826
49 - 58	-0.1073	-0.0015	0.0441	0.1816
51 - 56	0.1169	-0.0868	0.2667	0.1973
54 - 51	-0.1272	-0.1003	-0.112	-0.1132
56 - 51	-0.0308	-0.2077	0.0864	0.0611
57 - 9	-0.2684	0.1055	-0.2085	0.0797
58 - 49	-0.035	0.0196	0.0991	0.0338
59 - 11	-0.1106	0.0308	0.1666	-0.3603
60 - 47	-0.4389	-0.3465	-0.2162	-0.0087
61 - 13	-0.2825	-0.3042	-0.2492	-0.328

Caption: Deviation of J-coupling across hydrogen bond (J_{exp}-J_{comp}) backcalculated from cutoff or reaction field trajectories of GB3